sion of the scattering profile from various specimens by the molecular transform of type I collagen has yielded interference functions that all have a maximum at $1/1.42\ nm^{-1}$, but have various breadths. This indicates that, at closest approach, the molecules have the same nearest-neighbor separation in all of these tissues, a separation comparable to that found in the crystal structure. This finding suggests that the basic molecular interactions are the same in each of these tissues. The differing breadths of the intereference functions show that the variance in molecular position differs from one tissue to another, probably in inverse relation to the packing density. Whether this variance represents static or dynamic disorder is not yet known.

The disordered structures described above at the molecular level have an analog at the fibrillar level in tissues with relatively uniform diameter collagen fibrils, such as lamprey notochord sheath, lamprey skin, and embryonic tendons. From electron micrographs, one can compute the pair distribution function of the fibril locations and determine the degree of short- and long-range order (6). The degree of order seen is less than crystalline, but more correlated than the order of typical nematic liquid crystalline arrays which collagen fibrils resemble. Such tissues give a low-angle x-ray scattering pattern derived from the transform of the cylindrical fibrils multiplied by an interfibrillar interference function. These patterns can be analyzed to determine the diameter of the fully hydrated, native fibrils and their average nearest neighbor center-to-center separation.

Thus connective tissues contain rod-like fibrils which pack in partially correlated arrays in some tissues, and these in turn contain roughly cylindrical molecules that pack with crystalline or less exact lateral order. Calculation of the pair distribution functions from fiber x-ray diffraction data will allow a quantitative description of the lateral structure of these tissues at both the molecular and fibrillar levels and permit us to examine the influence of factors such as composition, ionic strength, pH, pressure, and temperature on these structures.

Received for publication 6 June 1985.

REFERENCES

1. Hulmes, D. J. S., and A. Miller. 1979. Quasi-hexagonal molecular packing in collagen fibrils. *Nature (Lond.)*. 282:878–880.
2. Fraser, R. D. B., and T. P. MacRae. 1981. Unit cell and molecular connectivity in tendon collagen. *Int. J. Biol. Macromol.* 3:193–200.
3. Fraser, R. D. B., T. P. MacRae, A. Miller, and E. Suzuki. 1983. Molecular conformation and packing in collagen fibrils. *J. Mol. Biol.* 167:497–521.
4. Eikenberry, E. F., B. Childs, S. B. Sheren, D. A. D. Parry, A. S. Craig, and B. Brodsky. 1984. Crystalline fibril structure of type II collagen in lamprey notochord sheath. *J. Mol. Biol.* 176:261–277.
5. Brodsky, B., E. F. Eikenberry, K. C. Belbruno, and K. Sterling. 1982. Variations in collagen fibril structure in tendon. *Biopolymers.* 21:935–951.
6. Eikenberry, E. F., B. Brodsky, A. S. Craig, and D. A. D. Parry. 1982. Collagen fibril morphology in developing chick metatarsal tendon: 2. Electron microscope studies. *Int. J. Biol. Macromol.* 4:393–398.

TWO-STRANDED α-HELICAL COILED-COILS OF FIBROUS PROTEINS

Theoretical Analysis of Supercoil Formation

ROBERT E. BRUCCOLERI,* JIRI NOVOTNY,* PETER KECK,‡ AND CHARLES COHEN‡
**Cellular and Molecular Research Laboratory, Massachusetts General Hospital and Harvard Medical School, Boston Massachusetts 02114; and ‡Creative BioMolecules Inc., Hopkinton Massachusetts 01748*

Left-handed "supercoils" (α-helical dimers) (1) are believed to be the dominant structural feature of fibrous proteins such as myosins, α-keratins, viral hemagglutinins, trypanosoma antigens, and cytoskeleton microfilaments and microtubules. Recent experimental work on synthetic oligoheptapeptides of increasing lengths (2) showed that peptides shorter than four repeats of the heptad sequence Lys-Leu-Glu-Ala-Leu-Glu-Gly have disordered structures in aqueous solutions, while longer peptides exist exclusively as α-helical dimers.

Using an empirical potential energy function that incorporates approximate corrections for solvent effects (3), we estimated the differences in Gibbs free energies of extended, α-helical and supercoiled peptides of increasing length. We also examined the effect of the current uncertainties in the calculation on the agreement to the experimentally observed trends of α-helix and supercoil stabilities. Such comparisons are an important first step in calibrating and testing an empirical Gibbs free energy function, which will be essential in the development of algorithms for the prediction of protein folding.

METHODS AND THEORY

Five polyheptapeptides (Ac-(Lys-Leu-Glu-Ala-Leu-Glu-Gly)$_n$-Lys-amide with n = 1–5) were constructed as extended β-strands, single α-helices, and supercoiled, parallel dimers (Fig. 1). The α-helices and

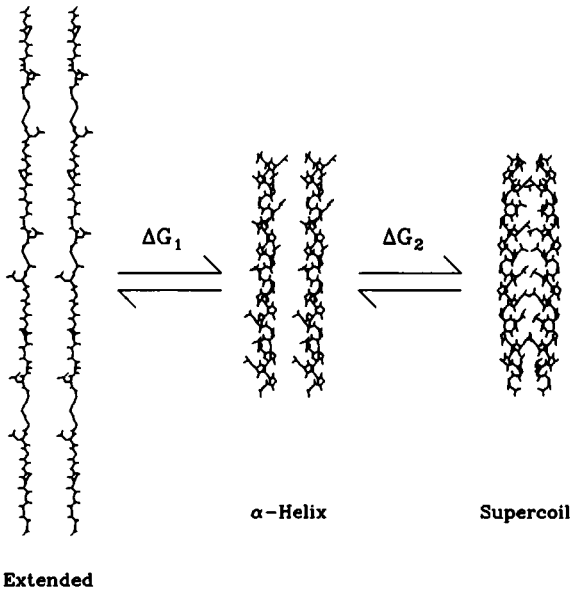

FIGURE 1 Stick figures for the three conformations of the peptide TM36, and relationship of the conformations and the free energy calculations. Only backbone atoms and leucine and alanine sidechains are shown, for reasons of clarity.

extended conformations were constructed using Pauling (4) ϕ, ψ values of $(-57°, -47°)$ and $(-120°, 140°)$, respectively. The supercoils were constructed starting with these α-helices, gently twisted to a pitch of 3.5 residues/turn, and then gently bent using the transformation (1),

$$\begin{bmatrix} x_h \\ y_h \\ z_h \end{bmatrix} = \begin{bmatrix} \cos\theta & -\sin\theta & 0 \\ \sin\theta & \cos\theta & 0 \\ 0 & 0 & 1 \end{bmatrix} \begin{bmatrix} x \\ y \\ z \end{bmatrix} + \begin{bmatrix} R\cos\theta \\ R\sin\theta \\ 0 \end{bmatrix}$$

where $\theta = (2\pi z/P)$, P is the supercoil pitch, and R is the supercoil radius. Crick's parameters for P (186 Å/turn) and R (5.2 Å) were used (1). Both manipulations do not preserve internal geometries; thus each twist or bend is performed in eight smaller steps with 10 cycles of ABNR energy minimization (5) following each transformation to restore the geometry (thus the term "gentle"). The sidechains are initially constructed using all-*trans* χ_i angles; once the dimer is formed, CONGEN, a program for searching the conformational space of polypeptides (6), is used to reconstruct the sidechains. To bury the leucine sidechains, which form a hydrophobic stripe on the α-helix, the α-helices were rotated "by hand" about the α-helix axis to direct the leucines toward the supercoil axis. This initial orientation was perturbed by a series of 10° rotations (in both directions), and the best orientation was selected by the lowest energy computed by CHARMM (5). The geometric energy terms (5) are nearly the same among all three structures; thus we assume no covalent energy differences.

The Gibbs free energy of a reaction, ΔG, represents a balance between differences in enthalpies and entropies of the reactants and reaction products: $\Delta G = \Delta H - T\Delta S$. The most important enthalpic contributions, ΔH, include differences in covalent, hydrogen bond, electrostatic and van der Waals energies. The predominant entropic contributions involve changes in solvent entropy at the solvent-solute interface (i.e., the hydrophobic force in aqueous solutions), loss of bond configurational entropy on attainment of compact structures (e.g., during folding or dimerization) and the decrease in molecular translational entropy on dimer formation. In our case, no changes in covalent energy occur. For the purpose of computation, we divided the Gibbs free energy of the dimer formation into two parts, namely, ΔG_1, the free energy of extended chain (random coil) to α-helix transition, and ΔG_2, the free energy of the dimerization calculated as follows:

$$\Delta G_1 = \Delta G_h + \Delta H_e + \Delta G_{HB} - T\Delta S_c,$$
$$\Delta G_2 = \Delta G_h + \Delta H_e - T\Delta S_c - T\Delta S_{TR}.$$

ΔG_h, which accounts for the solvent entropy differences (the hydrophobic force), was computed using the solvent-modified van der Waals energy (3). ΔH_e is the electrostatic energy difference calculated using Coulomb's law with a constant dielectric of 50 (7). The hydrogen bond energy differences, $\Delta G_{HB} = G(\text{peptide–peptide})_{HB} - G(\text{peptide–water})_{HB}$, were estimated as 1.0 kcal/bond based on recent experimental results of Fersht et al. (8). $T\Delta S_c$, the loss of configurational entropy, was estimated using the empirical formula $\Delta S_c = -R\log(3^N)$, where N is the number of bonds presumed to be rotationally hindered in the reaction products. For α-helix formation, the backbone torsions ϕ and ψ are fixed; thus $N = 2 \times$ number of residues. On dimer formation we assume partial hindrance of the buried leucine sidechains, and thus, we set N equal to the number of leucines in the interface. T is 300°K. Finally, $T\Delta S_{TR}$ specifies the loss of translational and rotational entropy on dimer formation from the two separate α-helical monomers, and an approximate value was taken from Jencks (9).

RESULTS AND DISCUSSION

Summary of the computed Gibbs free energy contributions is given in Table I. The transition to negative (i.e., favorable) values of the Gibbs free energy for the reaction, two peptides in random coils → α-helical supercoil (ΔG), occurs in the same range of peptide lengths as previously indicated by experiments (2). The free energy for random coil → α-helix transformation is generally zero, consistent

TABLE I
GIBBS FREE ENERGIES OF THE TRANSITION 2 RANDOM COILS → SUPERCOILED α-HELICES (KCAL/MOLE)

	2 Random Coils → α helices					2 Monomer helices → Supercoil				
Peptide*	ΔG_h	ΔH_e	ΔG_{HB}	$-T\Delta S_c$	ΔG_1	ΔG_h	ΔH_e	$-T\Delta S_c$	$-T\Delta S_{TR}$	$\Delta G^\ddagger$
TM8	−18.2	3.4	−12.0	21.0	−5.8	6.9	1.1	2.6	6.9	11.7
TM15	−19.6	7.4	−26.0	39.3	1.1	−2.4	0.2	5.2	6.9	11.0
TM22	−29.0	12.0	−40.0	57.6	0.6	−11.9	−3.4	7.9	6.9	0.1
TM29	−36.2	16.4	−54.0	76.0	2.2	−40.5	−4.2	10.5	6.9	−25.1
TM36	−54.0	21.6	−68.0	94.3	−6.1	−47.7	−4.4	13.1	6.9	−38.2

*Notation from reference 2—the number gives the peptide length.
‡$\Delta G = \Delta G_1 + \Delta G_2$

with the experimental data because no isolated α-helices of any length were detected. The peptide, TM8, is an exception, having a negative free energy, and it seems to be unrealistically affected by fluctuations in the computed ΔG_h values.

We stress that the values in Table I represent gross estimates, and the uncertainty in each term can affect the experimental agreement. Our estimates of the hydrophobic interaction, ΔG_h, are virtually identical to those obtained using the buried surface area rule of Chothia (10), i.e., 25 cal of $\Delta G/1$ Å^2 of buried surface. We justify a dielectric constant of 50 because nearly all the atoms in these structures are exposed to water, although it would be appropriate to reduce the dielectric constant for the buried atoms in the supercoil. Most applications of the CHARMM program (5) have used much smaller dielectric constants, which would greatly increase the magnitude of ΔH_e and would eliminate the calculated stability of the supercoil at any length. Variation of the hydrogen bond energy differences within the range cited by Fersht (0.5–1.5 kcal/mol/bond) can shift the length-dependent transition in either direction, as can a different estimate of the configurational entropy, although our estimates correspond to values given by Privalov (11). Finally, using the highest suggested value for the translational entropy loss, 11 kcal/mol, (9) would not greatly affect the experimental agreement.

Our calculation of the energetics of supercoiled α-helices compares well with experimental data. However, the considerable calculational uncertainties make it possible to achieve the same agreement with experiment using different and compensating assumptions. Thus, further comparisons of experimental data with calculations are necessary to improve and refine the empirical free energy function.

Received for publication 30 April 1985.

REFERENCES

1. Crick, F. H. C. 1953. The Fourier transform of a coiled-coil. *Acta Crystallogr.* 6:685–689.
2. Lau, S. Y. M., A. K. Taneja, and R. S. Hodges. 1984. Synthesis of a model protein of defined secondary and quaternary structure. Effect of chain length on the stabilization and formation of two-stranded α-helical coiled-coils. *J. Biol. Chem.* 259:13253–13261.
3. Novotny, J., R. E. Bruccoleri, and M. Karplus. 1984. An analysis of incorrectly folded protein models. Implications for structure predictions. *J. Mol. Biol.* 177:787–818.
4. Pauling, L., R. B. Corey, and H. R. Branson. 1951. The structure of proteins: two hydrogen-bonded helical configurations of the polypeptide chain. *Proc. Natl. Acad. Sci. USA.* 37:205–211.
5. Brooks, B. R., R. E. Bruccoleri, B. D. Olafson, D. J. States, S. Swaminathan, and M. Karplus. 1983. CHARMM: A program for macromolecular energy, minimization, and dynamics calculations. *J. Comput. Chem.* 4:187–217.
6. Bruccoleri, R. E. 1984. Macromolecular mechanics and protein folding. Ph.D. thesis, Harvard University.
7. Warshel, A., S. T. Russell, and A. K. Churg. 1984. Macroscopic models for studies of electrostatic interactions in proteins: limitations and applicability. *Proc. Natl. Acad. Sci. USA.* 81:4785–4789.
8. Fersht, A. R., J. P. Shi, J. Knill-Jones, D. M. Lowe, A. J. Wilkinson, D. M. Blow, P. Brick, P. Carter, M. M. Y. Waye, and G. Winter. 1985. Hydrogen bonding and biological specificity analysed by protein engineering. *Nature (Lond.).* 314:235–238.
9. Jencks, W. P. 1981. On the attribution and additivity of binding enzymes. *Proc. Natl. Acad. Sci. USA.* 78:4046–4050.
10. Chothia, C. 1975. Hydrophobic bonding and accessible surface area in proteins. *Nature (Lond.).* 248:338–339.
11. Privalov, P. L. 1979. Stability of proteins. Small globular proteins. *Adv. Prot. Chem.* 33:167–241.

CONFORMATIONAL AND ASSEMBLY PROPERTIES OF NUCLEOTIDE-DEPLETED TUBULIN

EDWARD J. MANSER AND PETER M. BAYLEY

Division of Physical Biochemistry, National Institute for Medical Research, London NW7 1AA, United Kindom

The reversible interaction of guanosine triphosphate (GTP) and guanosine diphosphate (GDP) with the exchangeable E-site of tubulin is central to mechanisms for GTP-supported microtubule assembly. High nucleotide affinities, with $K_a > 10^7$ M^{-1}, and protein instability hinder the study of nucleotide-depleted tubulin. We have, therefore, followed the removal of E-site GDP from microtubule (MT) protein and tubulin dimer with alkaline phosphatase, using HPLC to monitor nucleotide content, and near-ultraviolet (UV) circular dichroism (CD) to follow conformational properties.

We find that the conformational changes associated with nucleotide removal are reversible by adding GTP or GDP, and that GTP restores normal assembly. Most significantly, we show that pyrophosphate (3 mM) induces formation of microtubules from nucleotide-depleted tubulin in the absence of GTP, but does not restore the near-UV CD. We conclude that, contrary to the general view, e.g.